Crystal Structure of (Methyl 2-(methylamino)-1-cyclopentene-1-dithiocarboxylato-$\kappa N,\kappa S$)-carbonyl(triphenylphosphine)rhodium(I) and Kinetics of Iodomethane Oxidative Addition

Gideon J. J. Steyn, Andreas Roodt,* and Johann G. Leipoldt

Department of Chemistry, University of the Orange Free State, Bloemfontein 9300, Republic of South Africa

Received December 17, 1991

The preparation of the title complex, (methyl 2-(methylamino)-1-cyclopentene-1-dithiocarboxylato)carbonyl(triphenylphosphine)rhodium(I), is described. This complex, $C_{27}H_{27}NOS_2OPRh$, crystallizes in the monoclinic space group $P2_1/n$, with a = 15.665 (2) Å, b = 9.685 (1) Å, c = 18.166 (2) Å, β = 110.57 (1)°, Z = 4, and ρ_{calc} = 1.491 g cm^{-3}. A final R-value of 4.70% resulted from refinement of 4808 observed reflections. The title complex, in which triphenylphosphine is coordinated trans to the nitrogen atom of the methyl 2-(methylamino)-1-cyclopentene-1-dithiocarboxylato ligand (MACSM$^-$), undergoes oxidative addition with iodomethane with the formation of an alkyl intermediate, followed by carbonyl insertion with the formation of the corresponding Rh(III)–acyl complex. The reaction proceeds via an associative equilibrium followed by the methyl migration to form the acyl species according to the reaction

$$[Rh(MACSM)(CO)(PPh_3)] + CH_3I \underset{k_{-1}}{\overset{k_1, K_1}{\rightleftharpoons}} [RhI(MACSM)(PPh_3)(CO)(CH_3)] \xrightarrow{k_2} [RhI(MACSM)(PPh_3)(COCH_3)]$$

At 25.5 °C in $CHCl_3$ the equilibrium and forward and reverse rate constants for the first reaction were determined as 5 (1) M^{-1}, 3.4 (1) × 10^{-2} M^{-1} s^{-1}, and 8.6 (8) × 10^{-3} s^{-1}, and the limiting rate constant for the Rh(III)–acyl formation was determined as 8.1 (5) × 10^{-3} s^{-1}.

Introduction

The oxidative addition of iodomethane to rhodium(I) phosphine complexes is of importance in the Monsanto process[1] for the production of acetic acid. Since there are still some uncertainties in this mechanism, our group has been interested over the past few years in the manipulation of the reactivity of the Rh(I) center in the [Rh(BID)(CO)(PX$_3$)] type of complexes, where BID$^-$ = monocharged bidentate ligands such as acetylacetonate[2] and substituted acac ligands,[3] 8-hydroxyquinolinate,[4] cupferrate,[5] etc. containing different donor atoms such as oxygen, nitrogen, and sulfur[6] and PX$_3$ = different momodentate phosphine ligands with X = phenyl, *p*-chlorophenyl, *p*-methylphenyl, cyclohexyl, etc. The study of the products of these reactions (alkyl vs acyl) and the factors influencing the type of product is also of primary importance.

Previous papers[7] described solvent-dependence and high-pressure studies that were undertaken on the oxidative addition of iodomethane to [Rh(Sacac)(CO)(PPh$_3$)] (Sacac = thioacetylacetonate) to determine the nature of intermediates in these types of reactions. In these studies Scheme I was represented as the overall reaction, in which the acyl formation (k_2) was assumed to be rapid relative to that of the alkyl species (k_1) since it was experimentally found that the rate of disappearance of [Rh(Sacac)(CO)(PPh$_3$)] was the same as the rate of formation of the Rh(III)–acyl complex.

Scheme I

$$[Rh(BID)(CO)(PPH_3)] + CH_3I \underset{k_{-1}}{\overset{k_1, K_1}{\rightleftharpoons}} [RhI(BID)(PPh_3)(CO)(CH_3)] \xrightarrow{k_2} [RhI(BID)(PPh_3)(COCH_3)]$$

This paper describes the extension of this project to include bidentate ligands with the cyclopentenedithiocarboxylic acid backbone, containing both nitrogen and sulfur as donor atoms, in an attempt to increase the nucleophilicity of the Rh(I) center and therefore the activity of the complex toward oxidative addition.

Experimental Section

General Considerations. Unless otherwise stated, all chemicals were of reagent grade, and all preparations and measurements were carried out in air. The methyl ester of 2-(methylamino)-1-cyclopentene-2-dithiocarboxylic acid[8] (MACSMH) was prepared as described earlier. Infrared spectra were recorded on a Hitachi 270-50 instrument in KBr disks and $CHCl_3$, and NMR spectra were obtained on a Bruker 300-MHz spectrometer.

Preparation of Complexes. (Methyl 2-(methylamino)-1-cyclopentene-1-dithiocarboxylato)-$\kappa N,\kappa S$)dicarbonylrhodium(I), [Rh(MACSM)(CO)$_2$]. [Rh$_2$Cl$_2$(CO)$_4$] was prepared in situ by refluxing ca. 260 mg (1 mmol) of RhCl$_3$·3H$_2$O in 20 mL of DMF of ca. 30 min. The [Rh(MACSM)(CO)$_2$] complex was prepared by addition of 0.19 g (1 mmol) of the MACSMH ligand to the cooled DMF solution of [Rh$_2$Cl$_2$(CO)$_4$], followed by ca. 0.5 g of sodium acetate. After precipitation by ice-water and

(1) (a) Paulik, F. E. *Catal. Rev.* **1972**, *6*, 49. (b) Lowry, R. P.; Aguilo, A. *Hydrocarbon Process.* **1974**, *53*, 103.
(2) Basson, S. S.; Leipoldt, J. G.; Roodt, A.; Venter, J. A.; van der Walt, T. J. *Inorg. Chim. Acta* **1986**, *119*, 35.
(3) Basson, S. S.; Leipoldt, J. G.; Nel, J. T. *Inorg. Chim. Acta* **1984**, *84*, 167.
(4) Van Aswegen, K. G.; Leipoldt, J. G.; Potgieter, I. M.; Lamprecht, G. J.; Roodt, A.; van Zyl, G. J. *Transition Met. Chem.* **1991**, *16*, 369.
(5) Basson, S. S.; Leipoldt, J. G.; Roodt, A.; Venter, J. A. *Inorg. Chim. Acta* **1987**, *128*, 31.
(6) Leipoldt, J. G.; Basson, S. S.; Botha, L. J. *Inorg. Chim. Acta* **1990**, *168*, 215.
(7) Venter, J. A.; Leipoldt, J. G.; van Eldik, R. *Inorg. Chem.* **1991**, *30*, 2207 and references within.
(8) (a) Bordas, B.; Sohar, P.; Matolcsy, G.; Berencsi, P. *J. Org. Chem.* **1972**, *37*, 1727. (b) Nag, K.; Joardar, D. S. *Inorg. Chim. Acta* **1975**, *14*, 133.

0020-1669/92/1331-3477$03.00/0

Table I. Crystallographic Data for [Rh(MACSM)(CO)(PPh_3)]

formula	$C_{27}H_{27}NS_2OPRh$	V, Å^3	2580.4 (4)
fw	579.5	Z	4
cryst system	monoclinic	ρ_{calc}, g cm^{-3}	1.491
space group[a]	$P2_1/n$ (No. 14)	ρ_{expt}, g cm^{-3}	1.48
a, Å	15.665 (2)	T, °C	22
b, Å	9.685 (1)	μ, cm^{-1}	8.0
c, Å	18.166 (2)	cryst dimens, mm	0.30 × 0.180 × 0.10
β, deg	110.57 (1)		
R[b]	0.0470	no. of unique reflcns	6457
R_w[c]	0.0460		
λ(Mo Kα)	0.710 67	no. of obsd reflcns	4808 ($I > 3\sigma(I)$)

[a] Reference 9a. [b] $R = [(\Sigma\Delta F)/(\Sigma F_o)]$. [c] $R_w = [(\Sigma(\Delta F)^2)/(\Sigma(F_o)^2]^{0.5}$.

centrifuge a microcrystalline orange product was obtained (220 mg, yield > 60%). IR (KBr, cm^{-1}): (C≡O) 2050 (s), 1984 (s). ^{1}H NMR (C_3D_6O): δ 1.83 (m, 2 H, $-CH_{2(4)}$), 2.62 (s, 3 H, N–CH_3), 2.72 (t, 2 H, $-CH_{2(5)}$), 2.86 (t, 2 H, $-CH_{2(3)}$), 4.02 (s, 3 H, S–CH_3).

(Methyl 2-(methylamino)-1-cyclopentene-1-dithiocarboxylato-κ*N*,κ*S*)carbonyl(triphenylphosphine)rhodium(I), [Rh(MACSM)(CO)(PPh_3)]. To 5 mL of a cooled acetone solution containing 15 mg (0.05 mmol) of [Rh(MACSM)($CO)_2$] was added 13 mg (0.05 mmol) of PPh_3, resulting in the immediate evolution of CO gas. Slow evaporation (1–2 h) on ice produced orange diamond-shaped crystals of [Rh(MACSM)(CO)(PPh_3)], suitable for X-ray structure determination (22 mg, yield > 80%). Larger quantities of [Rh(MACSM)(CO)(PPh_3)] for kinetic measurements were obtained in the same way using ether instead as a result of the slow decomposition of the title complex in acetone solutions. IR (KBr, cm^{-1}): (C≡O) 1956 (s). ^{1}H NMR (C_3D_6O): δ 1.81 (m, 2 H, $-CH_{2(4)}$), 2.07 (s, 3 H, N–CH_3), 2.66 (t, 2 H, $-CH_{2(5)}$), 2.80 (t, 2 H, $-CH_{2(3)}$), 4.10 (s, 3 H, S–CH_3).

Kinetic Measurements. The rates of formation and disappearance of the different species were selectively monitored on a Hitachi 270–30 infrared spectrophotometer (equipped with a thermostated cell holder, ±0.2 °C) in chloroform as solvent since $CHCl_3$ does not exibit significant absorbance in the 1700–2300-cm^{-1} range. The observed first-order rate constants were obtained from least-squares fits of absorbance vs time data. [Rh(MACSM)(CO)(PPh_3)] decomposes in chloroform solutions, and care was therefore taken to dissolve a preweighed amount in the chloroform solutions already containing the required iodomethane and immediately starting the monitoring of the reaction. All reactions were monitored under pseudo-first-order conditions, with $[Rh]_{tot.} = 7 \times 10^{-3}$ M. The solid lines in Figures 3 and 4 represent the least-squares fits of the data (presented as points) to eqs 1 and 2, respectively.

Crystallography. Three-dimensional intensity data for the [Rh(MACSM)(CO)(PPh_3)] complex were collected on an Enraf-Nonius CAD-4F diffractometer with monochromated Mo Kα radiation. The structure was solved by the heavy-atom method, using the SHELX76 and -86 systems of programs.[9] Hydrogen atom positions were calculated as riding on the adjacent carbon atom with a C–H distance of 1.08 Å with the overall isotropic temperature factor being refined. The crystal data and intensity collection parameters are summarized in Table I.

Results and Discussion

NMR measurements showed that only one isomer of [Rh(MACSM)(CO)(PPh_3)] is formed in the reaction between [Rh(MACSM)($CO)_2$] and triphenylphosphine. The crystal structure determination was undertaken to determine the substitution mode in this complex.

Structure. The structure consists of discrete square-planar [Rh(MACSM)(CO)(PPh_3)] units of which the atom-numbering scheme is given in Figure 1. The fractional atomic coordinates and equivalent isotropic thermal parameters are given in Table II, and the most important bond distances and angles are reported in Table III.

This structure determination showed that in the reaction between [Rh(MACSM)($CO)_2$] and triphenylphosphine only one CO ligand is substituted by PPh_3, as was found in previous studies,[10] resulting in a square-planar orientation around the Rh(I) center. It was shown by these studies that the trans influence or structural trans effect (STE) for oxygen, nitrogen, and sulfur is in accordance with the electron negativity thereof, e.g., S > N > O, and it is therefore expected that the carbonyl ligand trans to the donor atom with the largest STE (i.e. sulfur) would primarily be substituted. Previous work[11] showed that the CO ligand that is displaced will in the five-coordinate transition state, together with the phosphine ligand and the bidentate ligand donor atom with the largest STE (in this case the sulfur atom), occupy the equatorial triangular plane. The nitrogen atom and the other carbonyl ligand will occupy the axial positions trans to one another, resulting in a final product with a *trans*-S–Rh–PPh_3 moiety. The

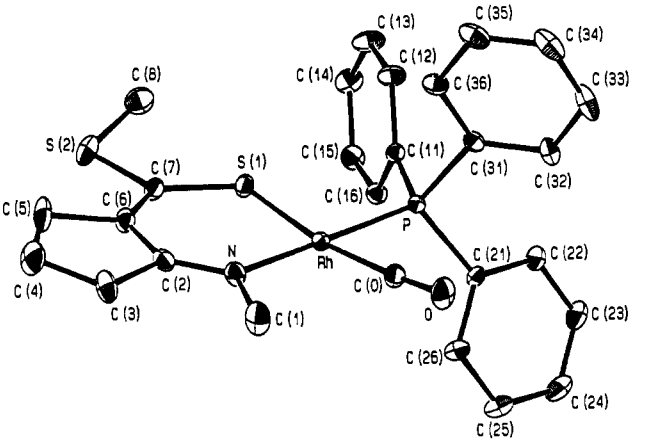

Figure 1. Atom-numbering scheme in [Rh(MACSM)(CO)(PPh_3)].

Table II. Fractional Atomic Coordinates (×10^4) and Equivalent Isotropic Thermal Parameters (Å^2 × 10^3) for [Rh(MACSM)(CO)(PPh_3)] with Esd's in Parentheses

	x/a	y/b	z/c	U_{eq}[a]
Rh	1655.2 (2)	2140.0 (4)	19.0 (2)	39.7 (1)
P	3031.6 (7)	1542.6 (13)	−36.8 (6)	38.0 (2)
S(1)	2425.9 (8)	3495.5 (15)	1083.6 (7)	51.2 (3)
S(2)	2186.7 (14)	5331.4 (21)	2309.7 (10)	84 (1)
C(11)	4058 (3)	2295 (5)	689 (2)	40 (1)
O	974 (3)	77 (5)	−1273 (3)	87 (1)
C(2)	173 (3)	3350 (6)	586 (3)	54 (1)
C(21)	3236 (3)	1947 (5()	−941 (2)	44 (1)
N	377 (3)	2607 (5)	72 (3)	55 (1)
C(0)	1202 (3)	902 (6)	−791 (3)	56 (1)
C(26)	2589 (4)	2707 (6)	−1522 (3)	60 (1)
C(31)	3165 (3)	−319 (5)	107 (3)	47 (1)
C(16)	4237 (3)	3604 (5)	550 (3)	50 (1)
C(6)	771 (4)	4091 (6)	1251 (3)	57 (1)
C(32)	2975 (4)	−847 (6)	745 (3)	59 (1)
C(7)	1698 (4)	4219 (6)	1492 (3)	54 (1)
C(12)	4525 (3)	1651 (6)	1396 (3)	63 (1)
C(15)	5040 (4)	4272 (6)	1114 (3)	61 (1)
C(36)	3369 (4)	−1224 (6)	−402 (4)	64 (1)
C(1)	−414 (4)	1983 (9)	−557 (4)	89 (2)
C(3)	−806 (4)	3550 (7)	560 (4)	77 (2)
C914)	5510 (4)	3627 (7)	1820 (3)	71 (2)
C(25)	2760 (5)	3121 (8)	−2189 (3)	80 (2)
C(13)	5244 (4)	2347 (7)	1952 (3)	76 (2)
C(22)	4058 (4)	1624 (6)	−1040 (3)	57 (1)
C(23)	4205 (5)	2032 (7)	−1716 (4)	71 (2)
C(35)	3359 (5)	−2645 (7)	−264 (5)	90 (2)
C(35)	3180 (4)	−3140 (7)	373 (6)	93 (2)
C(24)	3564 (5)	2764 (8)	−2286 (3)	80 (2)
C(33)	2997 (4)	−2245 (7)	873 (4)	77 (2)
C(4)	−729 (5)	4432 (11)	1251 (5)	113 (3)
C(5)	223 (5)	4749 (8)	1700 (4)	90 (2)

[a] $U_{eq} = {}^1/_3\Sigma_i\Sigma_j U_{ij} a_i^* a_j^* (a_i a_j)$.

(9) (a) Sheldrick, G. M. SHELX76. Program for crystal structure determination, University of Cambridge, England, 1976. (b) Sheldrick, G. M. *Acta Crystallogr.* **1990**, *A46*, 467. (c) *International Tables for X-ray Crystallography*; Riedel Publishing Co.: Dordrecht, The Netherlands, 1983; Vol. A, p 177.

(10) Graham, D. E.; Lamprecht, G. J.; Potgieter, I. M.; Roodt, A.; Leipoldt, J. G. *Transition Met. Chem.* **1991**, *16*, 193.

(11) Langford, C. H.; Gray, H. B. *Ligand Substitution Processes*; Benjamin: New York, 1965.

Table III. Selected Interatomic Bond Distances (Å) and Angles (deg) for [Rh(MASCM)(CO)(PPh$_3$)] with Esd's in Parentheses

Rh–P	2.269 (1)	Rh–S(1)	2.298 (1)
Rh–N	2.087 (4)	Rh–C(0)	1.836 (5)
P–C(11)	1.834 (4)	S(1)–C(7)	1.713 (5)
S(2)–C(7)	1.776 (5)	S(2)–C(8)	1.775 (7)
O–C(0)	1.146 (6)	C(2)–N	1.305 (6)
C(2)–C(6)	1.434 (8)	C(2)–C(3)	1.530 (7)
N–C(1)	1.488 (7)	C(6)–C(7)	1.367 (7)
C(6)–C(5)	1.516 (7)	C(3)–C(4)	1.488 (10)
C(4)–C(5)	1.459 (10)		
P–Rh–S(1)	87.5 (1)	P–Rh–N	177.7 (1)
S(1)–Rh–N	93.8 (1)	P–Rh–C(0)	84.5 (2)
S(1)–Rh–C(0)	171.2 (2)	N–Rh–C(0)	94.1 (2)
Rh–P–C(1)	118.2 (1)	Rh–S(1)–C(7)	111.4 (2)
N–C(2)–C(6)	128.8 (5)	N–C(2)–C(3)	122.9 (5)
C(6)–C(2)–C(3)	108.3 (5)	Rh–N–C(2)	129.3 (4)
Rh–N–C(1)	115.5 (3)	C(2)–N–C(1)	115.2 (4)
Rh–C(0)–O	175.2 (5)	C(2)–C(6)–C(7)	128.4 (5)
C(2)–C(6)–C(5)	109.7 (5)	C(7)–C(6)–C(5)	121.9 (5)
S(1)–C(7)–S(2)	117.0 (3)	S(1)–C(7)–C(6)	128.2 (4)
C(2)–C(7)–C(6)	114.8 (4)	C(2)–C(3)–C(4)	105.2 (5)
C(3)–C(4)–C(5)	110.9 (4)	C(6)–C(5)–C(5)	105.8 (6)

opposite substitution pattern was observed; i.e., the CO ligand trans to the nitrogen atom was substituted. This unexpected substitution mode can be attributed to the much larger steric demand of the methyl group on the nitrogen atom in the MACSM ligand, since it is expected that the TBP transition state with the sulfur atom in the apical position would be much more stable (less steric interaction with the PPh_3 than the nitrogen side of the MACSM ligand), in spite of having a larger electronic effect than the nitrogen. This substitution mode (some examples[12] are known in the literature) therefore seems to be sterically governed rather than electronically and is a significant observation if the weakening in the Rh–CO bond trans to the S-atom (discussed below) as a result of the large STE of sulfur is considered.

It was shown in the above-mentioned study[10] that the Rh–P bond distance in these types of [Rh(BID)(CO)(PPh$_3$)] complexes is an accurate indicator of the STE of the donor atoms in the bidentate ligand BID$^-$. In this structure the Rh–P bond length of 2.269 (1) Å observed is in the expected range when compared to the Rh–P (specifically for triphenylphosphine in these type of complexes) bond distances of 2.232 (2)–2.252 (2), 2.258 (2)–2.281 (2), and 2.278 (1)–2.300 (2) Å, respectively,[10,13] for oxygen, nitrogen, and sulfur donor atoms trans to the coordinated phosphine in five- and six-membered chelate ring systems. A direct correlation was also found between the bite angles in five- and six-membered chelate ring systems, where overlapping between the ligand orbitals and the dsp^2 orbitals of the Rh metal center is less effective in five-membered chelates (bite angle ca. 80°) compared to six-membered chelates (bite angle ca. 90°). The observed STE of the same ligand donor atoms in six-membered chelates was therefore found to be greater than in the corresponding five-membered systems. In this present study the S–Rh–N bite angle of 93.8 (1)° allows for good overlap between ligand and metal orbitals.

The Rh–N distance of 2.087 (4) Å compares well with the observed distances of 2.088 (6), 2.092 (7), and 2.098 (9) Å trans to triphenylphosphine in related [Rh(BID)(CO)(PPh$_3$)] complexes, containing nitrogen donor atoms in the bidentate ligands (BID$^-$ = 2-picolinate,[14] *N*-*o*-tolylsalicylaldiminate,[15] and 8-hydroxyquinolinate,[4] respectively). The Rh–CO bond length of 1.836 (5) Å, however, is significantly longer than that in similar complexes. In fact, the average Rh–CO bond in 14 complexes studied by our group over the past few years is 1.796 (8) Å.[10,16] In all these complexes the donor atom trans to the CO ligand was an oxygen atom. In this present study the carbonyl ligand is coordinated trans to a sulfur atom, thus underlining the large STE of sulfur, resulting in a significant increase in the Rh–CO bond distance from 1.796 (8) to 1.836 (5) Å. It is assumed that the increase in the nucleophilicity of the metal center (weaker Lewis acid) of the present MACSM system, compared to other [Rh(BID)(CO)(PPh$_3$)] complexes with oxygen donor atoms in BID$^-$, effectively decreases the σ-donating ability of the CO ligand thereby resulting in a weaker Rh–CO bond. However, the nucleophilicity of the Rh(I) center can still influence the carbonyl since electron density may be donated into the π^* orbitals of the CO ligand, decreasing the bonding order in the CO moiety and resulting in a weaker C–O bond. This reasoning is in direct agreement with the observed infrared data: ν(C≡O) in [Rh(MACSM)(CO)(PPh$_3$)] is 1956 cm^{-1} compared to values for ν(C≡O) of around 1980–2000 cm^{-1} for *trans*-O–Rh–CO moieties, demonstrating that the weakening of the Rh–CO bond is accompanied by a decrease in C≡O bond strength in this S–Rh–CO system. This interaction of the metal center in these systems will be discussed in a later paper. The increase in the nucleophilicity of the Rh(I) center in the present system is further manifested in the kinetic results discussed below.

The bond distances in the chelate ring N–C(2)–C(6)–C(7)–S(1) in [Rh(MACSM)(CO)(PPh$_3$)] show a definite shortening as a result of sp^2 character, the electron density being basically localized in bonds between the cyclopentene ring and the amino-nitrogen and the carboxylate-carbon atoms: N–C(2) = 1.305 (6) and C(6)–C(7) = 1.367 (7) Å. Evidence for this conclusion stems from comparative single bonds in the coordinated MACSM ligand (Table III): single C–C bonds (sp^3) of the range 1.459 (10)–1.530 (7) Å in the cyclopentene ring and bond distances of N–C(1) = 1.488 (7) and S(2)–C$_{av}$ = 1.776 (6) Å. This suggests a formal negative charge on the S(1) atom and underlines the excellent electron-donating capability thereof. The sp^2 character of the chelate ring is further demonstrated by the planarity thereof, the maximum deviation of any of the atoms forming the plane being <0.007 (7) Å, and is underlined by the small deviations for C(1) and S(2) therefrom (0.030 (9) and 0.105 (5) Å, respectively). The planes formed by the Rh-coordinated atoms and those forming the chelate ring are practically coplanar with the dihedral angle = 5.0 (2)°. The plane of the cyclopentene ring and that formed by the five chelate atoms do not differ significantly from coplanarity, the dihedral angle being 1.43 (5)°.

The crystal structure determination showed that the isomer that was formed in the reaction between [Rh(MACSM)(CO)(PPh$_3$)] and triphenylphosphine was not that initially expected, primarily due to steric factors. The supplementary ability of the nitrogen and sulfur atoms in this MACSM ligand system to increase the reactivity of the Rh(I) center toward oxidative addition is demonstrated and discussed below in the kinetic study.

Kinetics. Several studies[2,3,7] in the past few years by our group have demonstrated the formation of different products in the reactions between [Rh(BID)(CO)(PPh$_3$)] types of complexes and iodomethane. In the course of these studies products were isolated that showed that both cis and trans addition of the iodomethane may occur on the Rh center, forming the corresponding cis (as in the case of [RhI(cupf)(CO)(CH$_3$)(PPh$_3$)][5]) or trans ([RhI(ox)(CO)(CH$_3$)(PPh$_3$)][4]) alkyl species. Acyl complexes (e.g. [RhI(Sacac)(COCH$_3$)(PPh$_3$)][6,17,18]) were observed as primary products when the bidentate ligand contained a sulfur atom.

(12) Steynberg, E. C.; Lamprecht, G. J.; Leipoldt, J. G. *Inorg. Chim. Acta* **1987**, *133*, 33.
(13) Basson, S. S.; Leipoldt, J. G.; Roodt, A.; Preston, H. *Acta Crystallogr.*, in press.
(14) Leipoldt, J. G.; Lamprecht, G. J.; Graham, D. E. *Inorg. Chim. Acta* **1985**, *101*, 123.
(15) Leipoldt, J. G.; Basson, S. S.; Grobler, E. C.; Roodt, A. *Inorg. Chim. Acta* **1985**, *99*, 13.
(16) (a) Botha, L. J.; Basson, S. S.; Leipoldt, J. G. *Inorg. Chim. Acta* **1987**, *126*, 25. (b) Roodt, A.; Leipoldt, J. G.; Swarts, J. C.; Steyn, G. J. J. *Acta. Crystallogr.*, in press. (c) Leipoldt, J. G.; Grobler, E. C. *Inorg. Chim. Acta* **1982**, *60*, 141.
(17) Steyn, G. J. J.; Roodt, A.; Leipoldt, J. G. Manuscript to be submitted for publication in *Acta Crystallogr.*

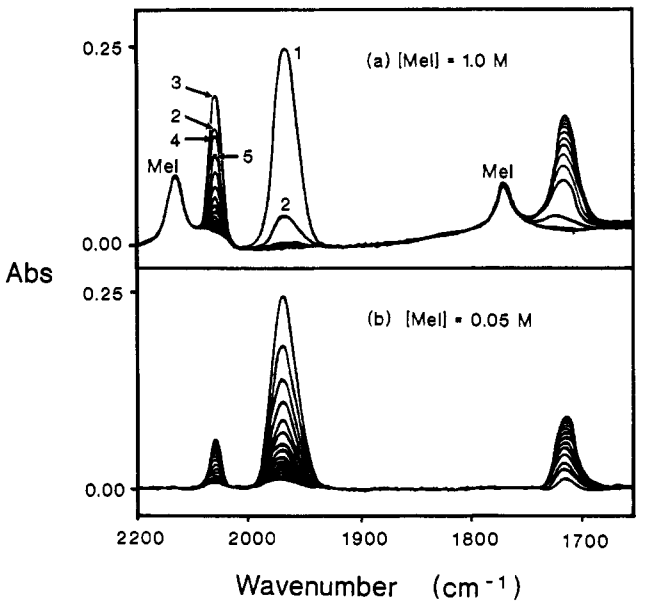

Figure 2. Repetitive IR scans (50-s intervals) for the oxidative-addition reaction of CH_3I to [Rh(MACSM)(CO)(PPh_3)] in $CHCl_3$ at 25.0 °C, $[Rh]_{tot.} = 7 \times 10^{-3}$ M, for (a) $[CH_3I] = 1.0$ M and (b) $[CH_3I] = 0.05$ M.

In this mentioned Sacac system the rate of disappearance of the Rh(I) complex was the same as the formation rate of the Rh(III)–acyl species, with only small amounts of the intermediate Rh(III)–alkyl species detectable. As a result of this, the formation and disappearance of the Rh(III)–alkyl species could not be studied. However, the introduction of the MACSM ligand to these systems has enabled us to selectively study the formation of both the intermediate Rh(III)–alkyl and the Rh(III)–acyl species. The formation of an acyl species (of which the crystal structure determination is underway) was confirmed to be the final product formed in this MACSM system; see Scheme I.

Figure 2 illustrates the observed reaction progress in the 1650–2100-cm^{-1} range at different iodomethane concentrations, as monitored by infrared spectroscopy. Figure 2a shows that the disappearance of the Rh(I)–carbonyl complex (signal at 1965 cm^{-1}) in 1.0 M [MeI] (k_{obsd} = 0.036 (3) s^{-1}) basically corresponds to the formation of the Rh(III)–alkyl species (rather strong peak at 2060 cm^{-1}) followed by the slow formation of the Rh(III)–acyl complex (k_{obsd} = 0.0057 (3) s^{-1}) at 1715 cm^{-1} (which in turn corresponds to the disappearance of the 2060-cm^{-1} signal). On the other hand, Figure 2b shows that at [MeI] = 0.05 M, the formation of the Rh(III)–alkyl species is less pronounced and more slowly and that the rate of disappearance of the Rh(I)–carbonyl complex in this case (k_{obsd} = 1.75 (5) × 10^{-3} s^{-1}) is the same as the formation rate of the Rh(III)–acyl species (k_{obsd} = 1.68 (5) × 10^{-3} s^{-1}). The observed rate of formation of the Rh(III)–alkyl complex was, at higher iodomethane concentrations, generally found to be a little higher than the disappearance rate of the Rh(I) complex since the formation of the Rh(III)–acyl species (and subsequent disappearance of the Rh(III)–alkyl complex) caused lower values for the absorbance at infinity (for Rh(III)–alkyl formation). It is however clear that the disappearance of [Rh(MACSM)(CO)(PPh_3)] is governed by the formation of the Rh(III)–alkyl species and subsequently by that of the Rh(III)–acyl complex and cannot be assigned to only one of the reactions over the concentration range [MeI] = 0.05–1.0 M.

Careful study of the Rh(III)–alkyl formation rate dependence on [MeI], as illustrated graphically in Figure 3, shows a direct relationship of the pseudo-first-order rate constant on [MeI],

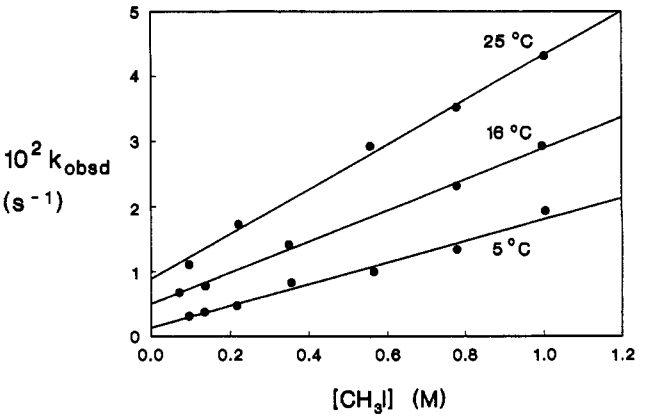

Figure 3. Temperature and $[CH_3I]$ dependence of the pseudo-first-order rate constant for the formation of [RhI(MACSM)(CO)(PPh_3)(CH_3)] (signal growth at ν = 2060 cm^{-1}) (Scheme 1) in $CHCl_3$, $[Rh]_{tot.} = 7 \times 10^{-3}$ M.

Table IV. Kinetic Results for the Reaction between [Rh(MACSM)(CO)(PPh_3)] and Iodomethane in Chloroform ($[Rh]_{tot.} = 7 \times 10^{-3}$ M)

const (Scheme I)	temp, °C	result
k_1,[a] M^{-1} s^{-1}	5.0	0.0167 (9)
	16.0	0.023 (1)
	25.5	0.034 (1)
$\Delta H^*(k_1)$, kJ mol^{-1}		23 (3)
$\Delta S^*(k_1)$, J K mol^{-1}		−195 (11)
k_{-1},[a] s^{-1}	5.0	0.0031 (5)
	16.0	0.0053 (4)
	25.5	0.0086 (8)
$\Delta H^*(k_{-1})$,kJ mol^{-1}		47 (12)
$\Delta S^*(k_{-1})$,J K mol^{-1}		−130 (4)
K_1,[b] M^{-1}	5.0	5 (1)
	16.0	4 (1)
	25.5	4 (1)
K_1,[c] M^{-1}	16.0	5 (1)
	20.5	6 (1)
	25.5	4 (1)
K_1,[d] M^{-1}	16.0	4 (1)
	20.5	5 (1)
	25.5	4 (1)
K_1,[e] M^{-1}	25.5	4 (1)
k_2,[c] s^{-1}	16.0	0.0027 (1)
	20.5	0.0036 (2)
	25.5	0.0076 (4)
k_2,[d] s^{-1}	16.0	0.0029 (2)
	20.5	0.0040 (3)
	25.5	0.0081 (5)
k_2,[e] s^{-1}	25.5	0.0083 (9)
$\Delta H^*(k_2)$, kJ mol^{-1}		70 (9)
$\Delta S^*(k_2)$, J K mol^{-1}		−40 (31)

[a] Formation of Rh(III)–alkyl species; Figure 3. [b] $K_1 = k_1/k_{-1}$; data in Figure 3. [c] From data in Figure 4 and eq 2. [d] Reference 19. [e] Formation of Rh(III)–acyl species; Figure 4 and eq 2.

with an observed intercept. The results from this study, consistent with the rate expression shown in eq 1 for an ordinary equilib-

$$k_{obs} = k_1[MeI] + k_{-1} \quad (1)$$

rium reaction, are reported in Table IV. Furthermore, the disappearance of the Rh(III)–alkyl peak corresponds exactly to the formation of the Rh(III)–acyl species; see Figure 4 (results at 25 °C). It is clear from Figure 4 that limiting kinetics prevail, for which the general rate expression (eq 2), consistent with a

$$k_{obsd} = \frac{k_2K_1[MeI]}{1 + K_1[MeI]} \quad (2)$$

fast equilibrium (K_1 = equilibrium constant) reaction followed by the second slow reaction with rate constant k_2, holds. This

(18) Cheng, C.-H.; Spivack, B. D.; Eisenberg, R. *J. Am. Chem. Soc.* **1977**, *99*, 3003.

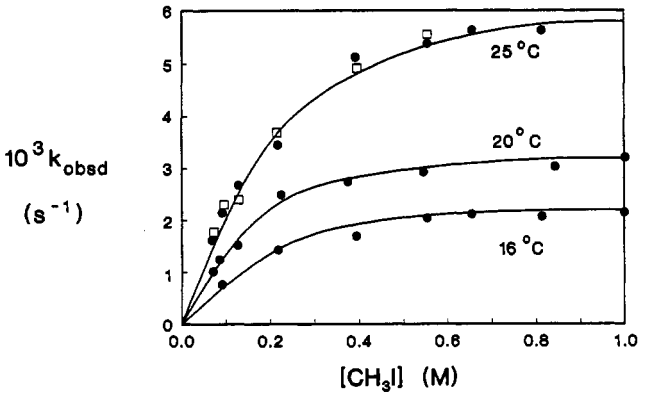

Figure 4. Temperature and [CH_3I] dependence of the pseudo-first-order rate constant for (a) the disappearance of [RhI(MACSM)(CO)-(PPh_3)(CH_3)] (decrease in signal at ν = 2060 cm^{-1}, circles) and (b) the formation of [RhI(MACSM)($COCH_3$)(PPh_3)] (signal growth ν = 1715 cm^{-1}, blocks) in $CHCl_3$, $[Rh]_{tot.}$ = 7 × 10^{-3} M.

expression suggests the observed linear relationship between $(k_{obsd})^{-1}$ and $([MeI])^{-1}$, which is indeed observed.[19] The results obtained from least-squares fits of the data shown in Figure 4 are shown in Table IV. Very important to note is the fact that the equilibrium constant K_1 obtained from both the data in Figure 3 ($K_1 = k_1/k_{-1}$) and those in Figure 4 (and from the inverse function of k_{obsd} vs [MeI][19]) are in excellent agreement.

A further important point worth noting is the fact that, under conditions where the Rh(III)–alkyl species is not present in significant amounts, first-order dependence in [MeI] will always be observed, with the second-order rate constant given by k_2K_1. This was observed in the oxidative addition[6,7] of iodomethane to [Rh(Sacac)(CO)(PPh_3)], but in this case it was assumed that the formation of the acyl species was rapid compared to that of the Rh(III)–alkyl species ($k_2 \gg k_1$ in Scheme I). The present study however suggests that the kinetics with the Sacac system might be governed by small K_1 values rather than k_2 being much larger than k_1.

The reported value for the Rh(III)–acyl formation in the [Rh-(Sacac)(CO)(PPh_3)] system at 25 °C in $CHCl_3$ is 0.0108 (2) M^{-1} s^{-1}.[5] If it is assumed that this second-order rate constant is actually given by k_2K_1 as observed for this system, it is clear from Table IV that the MACSM ligand increases the reactivity of the Rh(I) center toward oxidative addition by iodomethane ca. 4-fold to 0.040 (4) M^{-1} s^{-1} ($=k_2K_1$, where the average values for $k_2 = 8.1(2) \times 10^{-3}$ s^{-1} and $K_1 = 5$ (1) M^{-1} are assumed from Table IV), a significant increase. It is anticipated that manipulation of the substituents on these (N,S)-ligands may result in further useful reactivity tuning.

The activation parameters for both of the forward and reverse rate constants in the first equilibrium and that of the second acyl formation were calculated from the Eyring equation and are given in Table IV. The ΔH^* values are of the predicted magnitude[6] for these types of complexes whereas $\Delta S^*(k_1) = -195$ (11) J K mol^{-1} points to an expected associative pathway for the first step. The calculated $\Delta S^*(k_2)$ value of −40 (31) J K mol^{-1} is not a significant negative value and might be interpreted as being of the correct magnitude since acyl formation might demand less extreme changes in randomness than the usual associative systems. Further studies, which include detailed high-pressure investigations of the separate steps and solvent interaction with the different species in these types of oxidative-addition reactions, are required and planned to obtain more information on the mechanism of these systems.

Acknowledgment. Financial assistance by the South African FRD and the Research Fund of the University of the Orange Free State is gratefully acknowledged.

Supplementary Material Available: Listings of anisotropic thermal parameters, interatomic bond distances and angles, least-squares planes, calculated atomic coordinates for hydrogen atoms, and crystal and intensity collection data (9 pages). Ordering information is given on any current masthead page.

(19) Least-squares plots of $(1/k_{obsd}$ vs $1/[MeI])$ for the results shown in Figure 4 yield K_1 (intercept) and k_2 (slope) at different temperatures. The results are given in Table IV.